Nuclear Inst. and Methods in Physics Research B 480 (2020) 27–32

Contents lists available at ScienceDirect

Nuclear Inst. and Methods in Physics Research B

journal homepage: www.elsevier.com/locate/nimb

The surface of complex oxides; ion beam based analysis of energy materials

M. Niania[a], M. Sharpe[c], R. Webb[c], J.A. Kilner[a,b,*]

[a] Dept. of Materials, Faculty of Engineering, Imperial College, London SW7 2AZ, United Kingdom
[b] International Institute for Carbon Neutral Energy Research (I²CNER), 744 Motooka, Nishi-ku, Fukuoka 819-0395 Japan
[c] Ion Beam Centre, University of Surrey, Guildford, Surrey GU2 7XH, United Kingdom

ARTICLE INFO

Keywords:
SOFC cathodes
LEIS
Preferential sputtering
TRIDYN modelling
Ar depth profiling

ABSTRACT

LEIS depth profiles, obtained by low energy (0.5 keV) Ar^+ sputtering, have been analysed for the mixed conducting oxide material $La_{0.6}Sr_{0.4}Co_{0.2}Fe_{0.8}O_{3-\delta}$. Samples have been examined after differing thermal treatments to examine the sub-surface reorganisation of the cation species. The profiles have shown considerable changes, but these are not strongly correlated with the thermal treatments. The similarity between the profiles suggests that preferential sputtering effects can dominate the sub-surface region (~1–3 nm) where sputtering has not reached equilibrium. Preferential sputtering of oxygen in oxide materials is well known, but here we provide evidence of the preferential sputtering of the cationic species in a complex multicomponent oxide. Of note is strong enrichment (~30%) of the sputtered surface with the heaviest of the elements, La. Simulations using the code TRIDYN have confirmed the observations, in particular, La surface enrichment and the fluence needed to achieve steady state sputtering of $> 3 \times 10^{16}$ cm^{-2}.

1. Introduction

Materials for high temperature electrochemical devices, such as solid oxide fuel cells and electrolysers, (SOFCs and SOECs) have been under development for application in clean energy systems for many years [1,2]. Although acceptable performance can be achieved, the requirements of low cost and high durability have been a major hurdle to device commercialization. This has necessitated a lowering of operating temperatures from circa 800 °C to 900 °C, to temperatures in the region of 500 °C to 600 °C, with a consequent loss of electrochemical activity of the electrodes, particularly the cathode [3]. These cathodes are Mixed Ionic Electronic Conductors (MIECs) and are complex multicomponent ceramic materials usually based on the ABO_3 perovskite oxide structure. An example is the widely used material $La_{0.6}Sr_{0.4}Co_{0.2}Fe_{0.8}O_{3-\delta}$ (LSCF). Key to optimizing the performance of these devices is gaining an understanding of the gas/solid interface of the MIEC cathodes and how the structure, composition and activity evolves with time under operation.

To probe the surfaces of ceramic MIECs, such as LSCF, after treatment at temperature, a variety of surface sensitive techniques have been used [4,5] including ion beam based techniques such as Low Energy Ion Scattering (LEIS) to sample the composition of the outermost atomic layers [6–10] and SEM observations of the evolution of the surface [11]. Fig. 1 from ref [10] shows a cartoon of the typical surface termination and subsurface restructuring of an A'O substituted ABO_3 perovskite-based MIEC material found using LEIS analysis.

The aim of this work is to extend these previous studies to explore the effects of low energy Ar sputtering and how this will affect the interpretation and LEIS quantification of the composition of the altered region below the surface shown in Fig. 1. This has involved both Medium Energy Ion Scattering (MEIS) and time of flight SIMS depth profiling, in order to gain comparative information about the subsurface reorganisation and the transport of oxygen through these layers. Such comparative studies are very important for the interpretation of sputter depth profiling techniques, such as LEIS and XPS, where the sputtered surface is examined and not the sputtered flux, as in SIMS based techniques. An important aspect of this part of the study was to investigate any possible artefacts from the sputter depth profiling which might affect the interpretation of the LEIS signals, particularly in the first few nm sub surface, and a re-evaluation of the quantification method we have used for the LEIS data in previous publications (e.g. in [10]) described below. In that first attempt at a quantification method we understood that there would be significant preferential sputtering of the oxygen but quantified by assuming that the LEIS signal at the end of a LEIS depth profile, where the matrix signals were not changing, represented the cation composition of the bulk material. Using these levels and the known composition of the target sample, the signals were ratioed to represent deviations from stoichiometry. However, this

* Corresponding author at: Dept. of Materials, Faculty of Engineering, Imperial College, London SW7 2AZ, United Kingdom.
E-mail address: j.kilner@imperial.ac.uk (J.A. Kilner).

https://doi.org/10.1016/j.nimb.2020.07.022
Received 31 March 2020; Received in revised form 8 July 2020; Accepted 29 July 2020
Available online 28 August 2020
0168-583X/

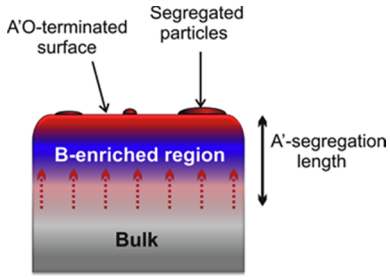

Fig. 1. Representation of the surface of a perovskite material after high temperature exposure in an oxidising atmosphere. Reproduced from Ref. [10] with permission from The Royal Society of Chemistry.

method ignores any preferential sputtering of the cations, and is clearly an approximation. Unfortunately, it was not apparent from the literature how significant any errors due to this approximation could be. Quantification of LEIS signals is not easy, but can be achieved by the use of standard elemental samples. However, with very reactive materials such as the rare earth and alkaline earth metals, it is difficult to get clean surfaces of any standard material. In addition, a recent publication has shown that, for La, there are possible matrix effects which can add to the complexity of quantifying the data [12]. Although there is significant literature on preferential sputtering of binary metal oxides [13–16], there have been few studies on the type of complex materials used as fuel cell cathodes [17,18].

One piece of evidence that is pertinent to this review is some earlier work on the related perovskite material $La_{0.6}Sr_{0.4}FeO_3$ (LSF) where XPS depth profiling was used with a 3 keV Ar^+ beam (angle of incidence not specified) to depth profile a thin film specimen [19]. The results of this analysis are shown below in Fig. 2. It is clear that there is a strong loss of oxygen and a corresponding build-up of the La as sputtering proceeds and this is evident up to a depth of almost 20 nm. The stoichiometric atomic fraction of La for this material is 0.12 and after sputtering to a depth of circa 20 nm the La surface fraction (as determined by XPS) has increased to ~ 0.3. The Sr signal shows a surface upturn, probably caused by Sr segregating to the surface during the preparation of the thin films, where the deposition temperature was 300 °C. However, the Sr signal remains mostly flat for the majority of the depth profile, even though it is slightly below the atomic fraction of 0.08 expected for this stoichiometry.

To gain an understanding of how these preferential sputtering

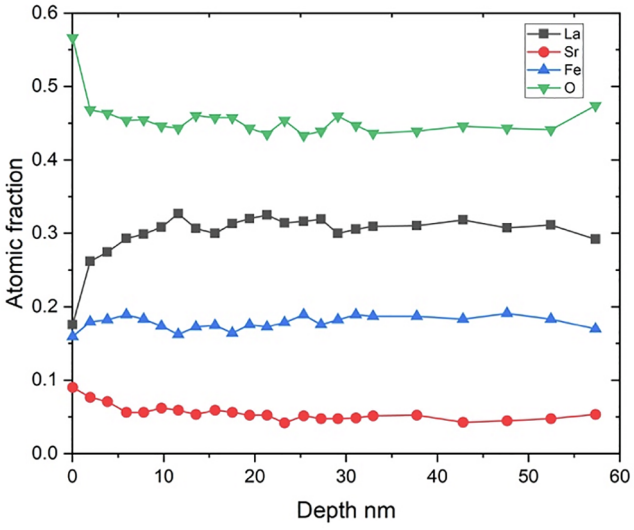

Fig. 2. XPS Sputter depth profile of a $La_{0.6}Sr_{0.4}FeO_3$ thin film (Ar^+ sputtering at 3 keV). Data taken from Ref. [19].

effects might affect a more complex material, such as LSCF, and the consequent problems of interpretation and quantification of LEIS depth profiling we have undertaken a study using both experimental and simulation techniques to estimate the effect and extent of cation preferential sputtering.

2. Experimental

Dense, flat and polished LSCF pellets were fabricated from commercially available Sigma Aldrich powder (lot MKBT7480V) as described in [20]. This was achieved by uniaxially pressing powder into 10 mm diameter discs at 2 tonnes, followed by an isostatic press at 250 MPa and sintering in air at 1250 °C. They were then sequentially ground using silicon carbide papers (P800, P1200, P2000) and polished using water based diamond suspensions (6 μm, 3 μm, 1 μm, 0.25 μm). Four samples were used, the heat treatments for each of these samples are shown in Table 1. The aim was to simulate various parts in the sequential stages of an isotope exchange experiment (e.g. as in [21]) using temperatures similar the operating conditions of an SOFC cathode.

This study is part of a broader investigation mentioned earlier where multiple ion-beam analysis techniques were used to analyse the sub-surface. LEIS depth profiling together with MEIS analysis were used to probe the sub-surface cation ratios. Each sample was analysed identically, except the exchanged sample, which received an additional LEIS and SIMS analysis in order to measure the oxygen isotopic tracer diffusion profile, these comparative studies are fully described in [20]. The LEIS depth profiles used as the focus of this study were obtained using an IONTOF QTAC 100 LEIS. Cation signals were measured using a 5 keV Ne^+ primary analysis beam at normal incidence and sputtering was achieved by a 0.5 keV Ar^+ sputter beam at 60° to the sample normal. The analysis raster area was 1000 × 1000μm with a beam current of ~ 5nA. 5 rounds of analysis were performed to improve measurement statistics which applied a fluence of 1.8×10^{13} atoms/cm^2 per analysis step.

2.1. Semi-Quantification of LEIS data

The purpose of this set of experiments was to determine the effect of preferential sputtering on the measurement of the material's sub-surface composition during the LEIS sputter depth profiling. The intensity of a LEIS peak for element *i*, S_i, is often presented in units of counts/nC. The expression governing this intensity is shown below [12].

$$S_i = \frac{1}{e}\xi R P_i^+ \left(\frac{d\sigma}{d\Omega}\right)_i N_i \quad (1)$$

where;

e is the electronic charge
R is a roughness factor
ξ is the analyser and detector instrumental factor
N_i is the atomic concentration in cm^{-2}
P_i^+ is the ion fraction after scattering by element i
$\left(\frac{d\sigma}{d\Omega}\right)_i$ is the differential cross section in Å/sr for element i

Many of these factors are unknown, but we can make the assumption that for a target with multiple elements that the factor $\frac{1}{e}\xi R$ remains the same for each element i under the same analytical conditions in the same instrument. The second set of factors, $P_i^+\left(\frac{d\sigma}{d\Omega}\right)_i$, will be element specific but for the purposes of obtaining trends we will at the moment neglect their effect. One point to note there is that the factor P_i^+ might be influenced by the expected loss of oxygen after the start of sputtering (seen in the XPS data above). Recent publications by Bruckner and coworkers [22,23] have shown the effect of the oxidation of pure metal surfaces can significantly affect the scattered intensity of the metal,

Table 1
Sample heat treatment summary.

Sample	Anneal Atmosphere	Anneal/Exchange Temp °C	Anneal time	Exchange time
As-polished	–	–	–	–
Pre-annealed	99.999% pure O_2	800	16 h	
Exchanged	99.999 pure O_2 followed by dry $^{18}O_2$	800	16 h	1 h
Air annealed	Ambient air	800	16 h	–

beyond that expected from the dilution of the metal surface density. For example, 5 keV He^+ scattering from Zn surfaces is reduced by a factor of approximately 3 times over that expected upon oxidation. It should be remarked that the change in oxygen content in the work reported by Bruckner et al. is very large compared to the expected change in oxygen content in these experiments, as indicated by the XPS results mentioned above (circa 25%). Hence any influence of the change in oxygen content should be minor. Given these caveats we can gain some relevant information about the trends in the surface concentrations of the cations as sputtering proceeds. To do this we must now look at the elements of the depth profile and do some normalisation. The signals for all the cations $S_i(x)$ at each point x in the depth profile can be summed, then each elemental signal can then be divided by this sum to give an intensity fraction $f_i(x)$ for element i.

$$f_i(x) = \frac{S_i(x)}{\sum_j S_j(x)} \tag{2}$$

3. Results and discussion

A typical LEIS spectrum for one of air annealed sample is shown below in Fig. 3, together with the components used to extract the relevant quantities needed. Clearly visible are the peaks corresponding to La and Sr, the scattering edges are marked on the figure. The integrated area under primary peaks of a LEIS spectra represents the quantity of ions scattered by a particular element (S_i). This intensity was extracted from each spectrum of the depth profile using the method described below.

As can be seen in Fig. 3, in a typical neon spectra there is a significant background component at the lower energies. This is a combination of ions scattered from atoms below the surface (also referred to as the 'in-depth' signal) and secondary ions generated by the scattering ions. Using the in-house IONTOF software, it is possible to account for the background by 1) subtracting an exponential component to remove secondary ions from the low energy signal and 2) using modified complementary error functions to model the 'in-depth' signal.

For each spectrum of the depth profile, the background varied slightly and so the exponential subtraction was adjusted on a per-spectra basis. In all cases, the exponential subtraction did not fully account for the all background. After the exponential subtraction, the remaining 'in-depth' background signal was modelled using modified complementary error functions that were applied to the lanthanum and strontium peaks (in this order) to fully subtract the background. This was not required for the cobalt and iron as the residual background was already negligible at this point. Each elemental peak could then be represented by a Gaussian distribution and these were fitted to calculate the integrated peak intensities. The peak position and peak width were held constant during the fitting process. It should be noted that the in-house IONTOF software automatically combines the complementary error function with a Gaussian peak. The parameters of the complementary error function are linked to the width of the corresponding Gaussian peak but the background intensity (the flat region) of the complementary error function was allowed to vary during the fitting process.

Moving now to consider the LEIS sputter depth profiling of the LSCF samples we can apply the assumptions made above to monitor trends in the LEIS signals. Fig. 4 shows an example of a LEIS depth profile for the "as-polished" sample, defined in Table 1. The sample was analysed using a 5 keV Ne^+ primary ion beam to give good resolution for the cation species but precludes the analysis of the oxygen. This sample was chosen as a first example because the material should, in principle, show a constant bulk composition across the whole depth profile (in the absence of preferential sputtering of the cation species). The depth profiling time was lengthened to ensure that steady state sputter

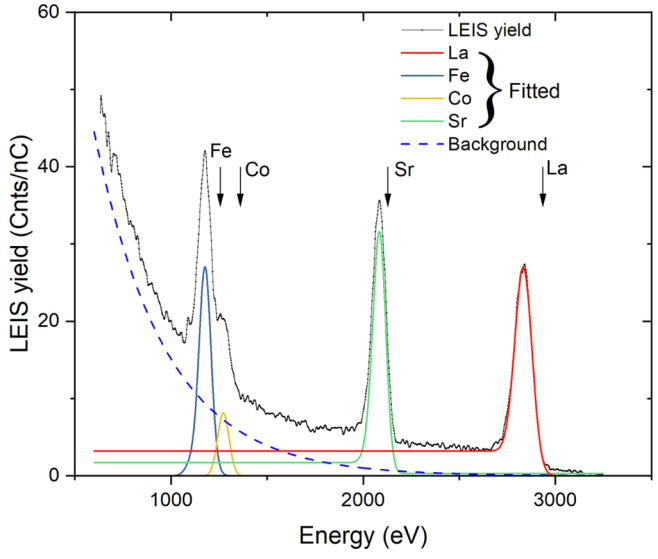

Fig. 3. LEIS spectrum of the air annealed sample obtained using a 5 keV Ne^+ primary beam at normal incidence. The scattering edge and fitted Gaussian components are shown for each of the elements. Also shown is the exponential background subtracted from the raw signal and the "in-depth" component used for the La and Sr Gaussian fits.

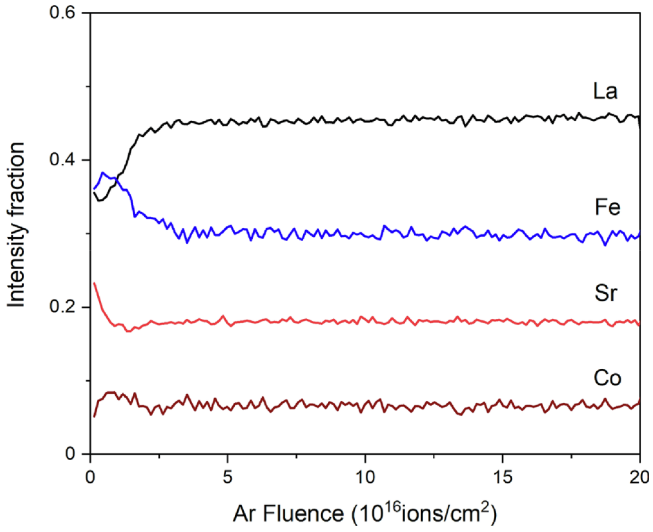

Fig. 4. LEIS depth profile of an as polished LSCF sample. For LEIS conditions see text.

conditions had been achieved and that the depth sampled was of the bulk composition by going much deeper than any expected inhomogeneities in the surface regions. The plateau region, seen at Ar^+ fluences of 10–20 $\times$ 10^{16} cm^{-2} ($\sim >$ 10 nm), in all the signals were taken to represent steady state sputtering.

Of note in Fig. 4 is that in the subsurface region there appears to be some considerable subsurface reorganisation of the cation species up to a fluence $>$ 3 $\times$ 10^{16} cm^{-2} (estimated $\sim$ 10–12 nm), past this point the signals remain constant. There is some similarity to the XPS profile of Fig. 2, particularly for the increase in the La signal, but in contrast the Fe signal has much more structure in the immediate sub-surface region. This behaviour is weakly followed by the Co signal and the Sr signal shows some evidence of Sr segregation towards the surface. Small scale reorganisation of the surface cations is possible in this as-polished sample but this should be limited to the very surface region, $<$ 1 nm because the diffusion coefficients at room temperature are so small [24]. The surface of this material has received no further heat treatment after sintering and being exposed during polishing, however the effect of the mechanical damage due to polishing may be enough to cause some small reorganisation of the immediate surface.

This unexpected profile prompted the investigation of the other materials that had seen heat treatments, as shown in Table 1, to determine if any other changes were apparent in these depth profiles. By heating the samples the cation diffusivities are considerably enhanced and reorganisation of the sub surface atoms, from that found in the as-polished state, of up to several nm is possible. Understanding the extent of any subsurface changes on heat treatment and, in particular, at temperature during long term service operation are important in understanding the evolution of the oxygen transport properties of these materials and their performance as an SOFC/SOEC electrode. The combined set of profiles are shown below in Fig. 5

The main difference in these profiles is the strong Sr segregation to the surface for the heat-treated samples, as has been noted in many previous publications. [8–11,25–28]. What is very clear is that there is a strong similarity in the shapes of all the profiles. The main features are;

- A marked increase in the La signal from the beginning of sputtering.
- A maximum in both the Fe and Co signals in the sub surface region (0 to 3 $\times$ $10^{16}cm^{-2}$)
- A small minimum in the Sr signal in the same region.
- Steady state is achieved for most signals at fluences $>$ 3 $\times$ 10^{16} cm^{-2}

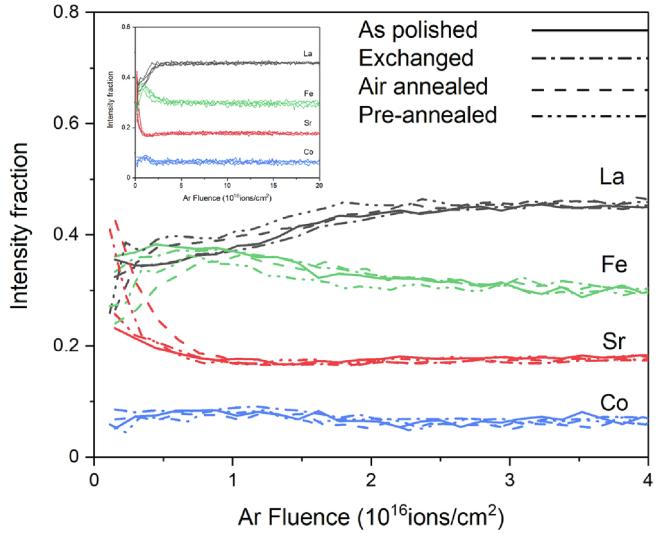

Fig. 5. LEIS depth profiles of all the samples in Table 1. The inset shows the depth profiles at much larger fluences to establish steady state conditions.

It appears most likely that these observations are a combination of the intrinsic cation distributions modified by the onset of preferential sputtering of the lighter B cations Fe and Co. The degree of the changes induced by preferential sputtering are, in principle quantifiable from the individual elemental profiles, neglecting any changes in the P_i^+ factors due to the loss of oxygen, however these changes are convoluted with any pre-existing changes due to cation reorganisation for the heat treated samples. Taking La as an example, for the heat treated samples the surface segregation of Sr will displace La on the A site of the perovskite structure and reduce its local concentration below that of the bulk, as seems apparent from the depth distribution of La and Sr for the air annealed sample in Fig. 5. Any increase in the sub-surface La signal upon sputter depth profiling is partially due to this replacement effect in addition to any effects of preferential sputtering. If we take the 'as polished' sample in Fig. 4 as an example where the Sr segregation, and hence this effect is minimised, the enrichment in the La signal is estimated to be $\sim$ 30%.

3.1. Simulation of preferential sputtering

In the literature there are several studies of binary oxides that detail the preferential sputtering of oxygen, but there are very few studies of complex oxides such as the perovskite materials used as SOFC cathodes. One of the problems of simulating MIEC materials such as LSCF is that the oxygen is very mobile (as is required for their application) and the oxides can exist in a wide range of oxygen stoichiometries, depending upon temperature and oxygen partial pressure. This high mobility and wide range of stoichiometry will have some effect upon the oxygen content of the bombarded material as oxygen lost by preferential sputtering can be readily replenished from the bulk.

Simulation of the Ar sputtering of LSCF under the conditions pertinent to the experimental conditions was performed using the TRIDYN 2019 code developed by W. Möller [29]. To reduce oxygen's influence and model the high oxygen mobility, due to limitations in the program, the density for oxygen and argon could only be increased by decreasing the density of the transition metals to a quarter of their values. After simulation, the depth was manually adjusted to only take into account the density of these transition metals. In the initial runs it was observed that heavy loss of oxygen occurred due to preferential sputtering and that the oxygen content dropped from a stoichiometry of 3 (atomic fraction 0.6) close to an oxygen stoichiometry of 1 (atomic fraction 0.33). This was deemed to be unrepresentative of the real material due to the effects of the high oxygen mobility mentioned earlier. It was then sought to fix the oxygen loss such that the oxygen stoichiometry reached a level shown by the XPS measurements of the very similar material LSF, reported in [19]. In that study the loss in oxygen is limited to an atomic fraction of 0.45 (oxygen stoichiometry 2.25). By altering the surface binding energies of the respective elements, it was found that the most effective method of limiting the oxygen loss was to increase the oxygen–oxygen surface binding energy to 5 eV. The other parameters used for the simulation are as follows: the surface binding energy of oxygen to the transition metals was set to 4 eV; the Ar ion energy was set to 0.5 keV at an angle of 60° from the normal. The surface composition was obtained by averaging the composition calculated by the simulation over the first 0.2 nm. It was felt that the implanted argon ions should not build up to a significant concentration and should be allowed to escape the system above a threshold value. This was set to 5% atomic fraction. Several different values were investigated which had little influence on the general results presented.

Fig. 6 above shows the result of this simulation. The similarities between the simulation of the surface composition and the signals obtained by LEIS are immediately apparent. There is a significant enrichment of the surface in lanthanum, however, there is no evidence of the sub surface peaking of the B cations Fe and Co. The calculated enrichment of La is $\sim$ 20%, which may be a slight underestimation when compared to the $\sim$ 30% found experimentally. The Sr signal, as

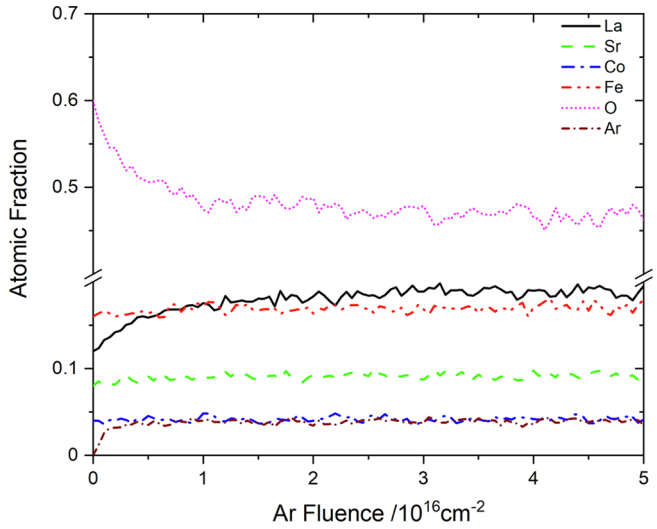

Fig. 6. TRIDYN simulation of the immediate surface composition after 0.5 eV Ar sputtering of an LSFC as polished sample.

seen in the XPS profile, is relatively unaffected by the sputtering. It is thus highly likely that the features seen in the Fe, Co and, in particular, the Sr LEIS signals in Fig. 5 are due to compositional changes in the samples due to the heat treatment. The other main feature of the simulation is that the establishment of sputtering steady state for the cation species at a fluence $\sim 3 \times 10^{16}$ cm^{-2}. This is comparable to the Ar fluence reported for earlier published LEIS depth profiles [6–11,27,28]. It is evident that any depth profiles presented in these earlier works, calibrated using the bulk cation stoichiometry and the steady state LEIS signal levels, will be subjected to some distortion due to preferential sputtering effects.

It remains difficult so see how any surface sensitive sputter depth profile technique can be used to unfold the changes in composition that occur in these very shallow depths. This, unfortunately, is the very region where steady state sputtering is being established and changes in surface composition are inevitable. One final note is that, despite these problems, LEIS was successfully used to show the changes in the surface composition of a Ruddlesden Popper phase $(La_{1-x}Sr_x)_2CoO_4$ thin film. Cation ratios measure by LEIS showed a shallow region of different cation composition to the bulk. This turned out to be 2 unit cells of the perovskite phase $(La_{1-x}Sr_x)CoO_3$ formed epitaxially on the surface of this material which was later revealed by high resolution cross-sectional TEM [28] emphasising the effectiveness of use complementary techniques to aid with interpretation.

4. Conclusions

The experiments and simulation presented here report the first detailed study of the effects of sputtering on the surface composition of a complex oxide. It is clear that preferential sputtering affects the surface composition of these materials and this is very important for the interpretation of sputter depth profiling techniques, such as LEIS and XPS, where the sputtered surface is examined and not the sputtered flux, as in SIMS based techniques. It is clear that preferential sputtering of the lightest component oxygen is severe, this is highlighted in the TRIDYN simulations. It is also clear that the cation species are subject to preferential sputtering, this is not surprising as this is essentially a phenomenon governed by the mass of the target atoms, however this has not been documented before in complex oxide systems. The implications of this finding is that simple quantification systems such as those reported in ref [10] are not accurate and can lead to significant errors. It remains a challenge to reveal the subtle changes that must occur in the subsurface regions of these oxides at temperature by using any one analytical depth profiling technique. Any technique using sputtering to depth profile (such as LEIS), is likely to suffer from the problem noted here: that compositional changes in the immediate sub-surface region will also be influenced by preferential sputtering whilst sputter equilibrium is established.

Declaration of Competing Interest

The authors declare that they have no known competing financial interests or personal relationships that could have appeared to influence the work reported in this paper.

Acknowledgements

The authors would like to acknowledge the support of JSPS/EPSRC (EP/P026478/1) Core-to-Core Program (Advanced Research Networks) “Solid Oxide Interfaces for Faster Ion Transport (SOIFIT)” and the support by World Premier International Research Center Initiative (WPI), Ministry of Education, Culture, Sports, Science, and Technology of Japan (MEXT), Japan.

References

[1] N. Minh, Solid oxide fuel cell technology? features and applications, Solid State Ionics 174 (2004) 271–277, https://doi.org/10.1016/j.ssi.2004.07.042.
[2] J.A. Kilner, M. Burriel, Materials for Intermediate-Temperature Solid-Oxide Fuel Cells, Annu. Rev. Mater. Res. 44 (2014) 365–393, https://doi.org/10.1146/annurev-matsci-070813-113426.
[3] Z. Gao, L.V. Mogni, E.C. Miller, J.G. Railsback, S.A. Barnett, A perspective on low-temperature solid oxide fuel cells, Energy Environ. Sci. 9 (2016) 1602–1644, https://doi.org/10.1039/c5ee03858h.
[4] J. Kuyyalil, D. Newby, J. Laverock, Y. Yu, D. Cetin, S.N. Basu, K. Ludwig, K.E. Smith, Vacancy assisted SrO formation on La0.8Sr0.2Co0.2Fe0.8O3 − δ surfaces—A synchrotron photoemission study, Surf. Sci. 642 (2015) 33–38, https://doi.org/10.1016/j.susc.2015.08.001.
[5] A.-K. Huber, M. Falk, M. Rohnke, B. Luerssen, M. Amati, L. Gregoratti, D. Hesse, J. Janek, In situ study of activation and de-activation of LSM fuel cell cathodes – Electrochemistry and surface analysis of thin-film electrodes, J. Catal. 294 (2012) 79–88, https://doi.org/10.1016/j.jcat.2012.07.010.
[6] A. Limbeck, G.M. Rupp, M. Kubicek, H. Téllez, J. Druce, T. Ishihara, J.A. Kilner, J. Fleig, Dynamic etching of soluble surface layers with on-line inductively coupled plasma mass spectrometry detection – a novel approach for determination of complex metal oxide surface cation stoichiometry, J. Anal. At. Spectrom. 31 (2016) 1638–1646, https://doi.org/10.1039/c6ja00154h.
[7] J. Druce, H. Tellez, T. Ishihara, J.A. Kilner, Surface Composition and Oxygen Exchange Properties of Alkaline Earth-Free Perovskites; LaCo0.6Ni0.4O3, Ionic and Mixed Conducting Ceramics 10 (2016) 71–80, https://doi.org/10.1149/07207.0071ecst.
[8] H. Tellez, J. Druce, J.A. Kilner, T. Ishihara, Relating surface chemistry and oxygen surface exchange in LnBaCo2O(5 + delta) air electrodes, Faraday Discuss. 182 (2015) 145–157, https://doi.org/10.1039/c5fd00027k.
[9] G.M. Rupp, H. Téllez, J. Druce, A. Limbeck, T. Ishihara, J. Kilner, J. Fleig, Surface chemistry of La0.6Sr0.4CoO3 − δ thin films and its impact on the oxygen surface exchange resistance, J. Mater. Chem. A 3 (2015) 22759–22769, https://doi.org/10.1039/c5ta05279c.
[10] J. Druce, H. Téllez, M. Burriel, M.D. Sharp, L.J. Fawcett, S.N. Cook, D.S. McPhail, T. Ishihara, H.H. Brongersma, J.A. Kilner, Surface termination and subsurface restructuring of perovskite-based solid oxide electrode materials, Energy Environ. Sci. 7 (2014) 3593–3599, https://doi.org/10.1039/c4ee01497a.
[11] M. Niania, R. Podor, T.B. Britton, C. Li, S.J. Cooper, N. Svetkov, S. Skinner, J. Kilner, In situ study of strontium segregation in La0.6Sr0.4Co0.2Fe0.8O3 − δ in ambient atmospheres using high-temperature environmental scanning electron microscopy, J. Mater. Chem. A 6 (2018) 14120–14135, https://doi.org/10.1039/c8ta01341a.
[12] A.A. Zameshin, A.E. Yakshin, J.M. Sturm, H.H. Brongerma, F. Bijkerk, Double matrix effect in low energy ion scattering from La surfaces, Appl. Surf. Sci. 440 (2018) 570–579, https://doi.org/10.1016/j.apsusc.2018.01.174.
[13] E. Watanabe, M. Yoshinari, Changes in X-ray photoelectron spectra of yttria-tetragonal zirconia polycrystal by ion sputtering, Appl. Phys. A 122 (2016), https://doi.org/10.1007/s00339-016-9930-0.
[14] G.D. Wang, D.D. Kong, Y.H. Pan, H.B. Pan, J.F. Zhu, Low energy Ar-ion bombardment effects on the CeO2 surface, Appl. Surf. Sci. 258 (2012) 2057–2061, https://doi.org/10.1016/j.apsusc.2011.04.103.
[15] M.P. Seah, T.S. Nunney, Sputtering yields of compounds using argon ions, J. Phys. D Appl. Phys. 43 (2010), https://doi.org/10.1088/0022-3727/43/25/253001.
[16] T. Kubart, T. Nyberg, S. Berg, Modelling of low energy ion sputtering from oxide surfaces, J. Phys. D Appl. Phys. 43 (2010) 205204, , https://doi.org/10.1088/0022-3727/43/20/205204.

[17] B. Psiuk, J. Szade, K. Szot, SrTiO3 surface modification upon low energy Ar+ bombardment studied by XPS, Vacuum 131 (2016) 14–21, https://doi.org/10.1016/j.vacuum.2016.05.026.
[18] M.E. Twigg, L.M.B. Alldredge, W. Chang, A. Podpirka, S.W. Kirchoefer, J.M. Pond, Structure and composition of Ba0.5Sr0.5TiO3 films deposited on (001) MgO substrates and the influence of sputtering pressure, Thin Solid Films 548 (2013) 178–185, https://doi.org/10.1016/j.tsf.2013.09.057.
[19] T. Götsch, D. Hauser, N. Köpfle, J. Bernardi, B. Klötzer, S. Penner, Complex oxide thin films: Pyrochlore, defect fluorite and perovskite model systems for structural, spectroscopic and catalytic studies, Appl. Surf. Sci. 452 (2018) 190–200, https://doi.org/10.1016/j.apsusc.2018.05.019.
[20] A.R.M. Niania, J. van Den Berg, J.A. Kilner, The effect of sub-surface strontium depletion on oxygen diffusion in La0.6Sr0.4Co0.2Fe0.8O3-δ, J. Mater. Chem. A (2020) (Submitted for publication).
[21] Z. Shen, S.J. Skinner, J.A. Kilner, Oxygen transport and surface exchange mechanisms in LSCrF-ScCeSZ dual-phase ceramics, PCCP 21 (2019) 13194–13206, https://doi.org/10.1039/c9cp02175b.
[22] B. Bruckner, P. Bauer, D. Primetzhofer, Neutralization of slow helium ions scattered from single crystalline aluminum and tantalum surfaces and their oxides, Surf. Sci. 691 (2020) 121491, , https://doi.org/10.1016/j.susc.2019.121491.
[23] B. Bruckner, P. Bauer, D. Primetzhofer, The impact of surface oxidation on energy spectra of keV ions scattered from transition metals, Appl. Surf. Sci. 479 (2019) 1287–1292, https://doi.org/10.1016/j.apsusc.2018.12.210.
[24] M. Kubicek, G.M. Rupp, S. Huber, A. Penn, A.K. Opitz, J. Bernardi, M. Stoger-Pollach, H. Hutter, J. Fleig, Cation diffusion in La(0.6)Sr(0.4)CoO(3-delta) below 800 degrees C and its relevance for Sr segregation, PCCP 16 (2014) 2715–2726, https://doi.org/10.1039/c3cp51906f.
[25] K.T. Wu, H. Téllez, J. Druce, M. Burriel, F. Yang, D.W. McComb, T. Ishihara, J.A. Kilner, S.J. Skinner, Surface chemistry and restructuring in thin-film Lan+1NinO3n+1 (n = 1, 2 and 3) Ruddlesden-Popper oxides, J. Mater. Chem. A 5 (2017) 9003–9013, https://doi.org/10.1039/c7ta01781b.
[26] H. Tellez, J. Druce, T. Ishihara, J.A. Kilner, Effects of Microstructure on Surface Segregation: Role of Grain Boundaries, in: M.B. Mogensen, T. Kawada, T.M. Gur, X.D. Zhou, A. Manivannan (Eds.), Ionic and Mixed Conducting Ceramics, 2016, pp. 57–69, , https://doi.org/10.1149/07207.0057ecst.
[27] M. Burriel, H. Téllez, R.J. Chater, R. Castaing, P. Veber, M. Zaghrioui, T. Ishihara, J.A. Kilner, J.-M. Bassat, Influence of crystal orientation and annealing on the oxygen diffusion and surface exchange of La2NiO4+δ, J. Phys. Chem. C 120 (2016) 17927–17938, https://doi.org/10.1021/acs.jpcc.6b05666.
[28] Y. Chen, H. Téllez, M. Burriel, F. Yang, N. Tsvetkov, Z. Cai, D.W. McComb, J.A. Kilner, B. Yildiz, Segregated chemistry and structure on (001) and (100) surfaces of (La1−xSrx)2CoO4 override the crystal anisotropy in oxygen exchange kinetics, Chem. Mater. 27 (2015) 5436–5450, https://doi.org/10.1021/acs.chemmater.5b02292.
[29] W. Möller, W. Eckstein, Tridyn — A TRIM simulation code including dynamic composition changes, Nucl. Instrum. Methods Phys. Res., Sect. B 2 (1984) 814–818, https://doi.org/10.1016/0168-583x(84)90321-5.